FAULT DIAGNOSIS AND DECISION SUPPORT SYSTEM FOR POWER GRIDS BASED ON DATA AND KNOWLEDGE

Xiaogang WU[1]*, Qingbiao LIN[2], Shengmin QIU[3], Yan GUO[4], Xingwang CHEN[5], Zhizhong LI[6]

The decision-making process for power grid faults involves multiple dimensions of information. Effectively integrating this information and achieving intelligent optimization are essential for improving power grid security. Traditional fault diagnosis relies on a single data source and often lacks accuracy in complex fault scenarios. This study puts forward an intelligent optimization algorithm for power grid fault decision-making. The algorithm integrates Semantic Vector Extraction optimized by Particle Swarm Optimization, One-Dimensional Convolutional Neural Network, and Long Short-Term Memory network optimized by Grey Wolf Optimizer. It combines power grid model calculation with logical reasoning to enable fast and accurate decision-making in fault scenarios through optimization algorithms. Experimental results show that the proposed model achieves an average correct classification rate of 96% across five types of faults, with an average accuracy of 94% in various operations, an average response time of 116 ms, and an average CPU usage of 26%. These findings indicate that the algorithm put forward effectively shortens the fault response time while improving the overall security of power grid operations. It effectively addresses the low diagnostic accuracy of traditional methods in complex fault scenarios and provides new ideas and approaches for maintaining grid security. This contributes to the development of intelligent and efficient power grid operations.

Keywords: Power grid fault diagnosis, Decision support system, Multi-source data integration, Knowledge-driven, Intelligent optimization

[1]* Power Dispatching Control Center, China Southern Power Grid Company Ltd. (CSG), Guangzhou, Guangdong 510000, China, corresponding author, e-mail: wxg1234560813@163.com
[2] Power Dispatching Control Center, China Southern Power Grid Company Ltd. (CSG), Guangzhou, Guangdong 510000, China
[3] Power Dispatching Control Center, China Southern Power Grid Company Ltd. (CSG), Guangzhou, Guangdong 510000, China
[4] Power Dispatching Control Center, China Southern Power Grid Company Ltd. (CSG), Guangzhou, Guangdong 510000, China
[5] Power Dispatching Control Center, China Southern Power Grid Company Ltd. (CSG), Guangzhou, Guangdong 510000, China
[6] Power Dispatching Control Center, China Southern Power Grid Company Ltd. (CSG), Guangzhou, Guangdong 510000, China

1. Introduction

As power systems continue to expand in scale and integrate a high share of renewable energy, the grid's operating environment has grown increasingly complex, leading to a notable rise in both the likelihood of faults and the extent of their impact [1]. Rapidly and accurately diagnosing faults and formulating optimal handling strategies are a crucial factor in maintaining the security and stability of power grid operations. When faced with the need to integrate multi-source heterogeneous data, traditional fault diagnosis exposes the shortcomings of insufficient data processing capabilities. Existing decision support systems are mostly based on static rule bases or single optimization objectives, which are difficult to adapt to the multi-objective collaborative optimization needs such as reliability improvement, economic optimization, and power supply continuity guarantee in the dynamic operation environment of the power grid. When dealing with dynamic conditions such as load fluctuations and new energy grid connection, the timeliness and comprehensive benefits of strategy formulation are both challenged. 1D Convolutional Neural Network (1D-CNN) can efficiently extract transient characteristics of power grid faults through one-dimensional convolution kernels and realize local mutation detection [2]. Grey Wolf Optimizer (GWO)optimizes Long Short-Term Memory (LSTM)to solve the defect that traditional models are not able to fit complex state processes [3]. Particle Swarm Optimization (PSO)optimization of Semantic Vector Extraction (SVE)can integrate particle swarm multi-objective optimization and semantic vector analysis to form a technical closed loop from accurate fault diagnosis to transparent decision support [4,5]. Therefore, the study proposes a decision support system that combines PSO-SVE, 1D-CNN and GWO-LSTM, hoping to reduce the fault response time while enhancing the safety of power grid operation. The innovation of the study is that through algorithm fusion, a power grid fault diagnosis and decision support system that takes into account accuracy, real-time and explainability is constructed.

2. Related Works

As the scale of power systems expands, the operating environment of power grids becomes more complex. Traditional diagnostic methods cannot meet the diagnosis and decision-making needs in complex fault scenarios. With the swift advancement of artificial intelligence technologies, researchers both domestically and internationally have explored its potential, aiming to incorporate it into conventional diagnostic approaches [6]. Almulhim and Barahona introduced a decision support framework grounded in fuzzy theory combined with multi-criteria decision analysis principles. By integrating 16 critical indicators and accounting for both decision-makers' hesitation and experiential knowledge, the system delivers dependable outcomes. It proves effective in addressing complex and unstructured challenges within this domain [7]. Shahraki et al. developed a decision support system for field problems such as complex and time-consuming intern schedules. They used mixed integer linear programming to develop a scheduling model to optimize daily tasks and monthly rotation arrangements [8]. Bazilevych et al. proposed an intelligent information system to support decision-making in epidemiological diagnosis. Their method analyzed incidence data and modeled the epidemic process to identify decision-making features. They also developed the system's model and architecture to support epidemiological decision-making [9]. Lu focused on the challenges of telemedicine decision support in elderly healthcare management. They designed a knowledge discovery-based decision support system that used digital information extraction to construct a utilization modeling method. By combining simulation analysis, they modeled system functionality and morphological features, fitting Non-Uniform Rational B-Splines curves to build surface models [10]. Mufana and Ibrahim developed an information system for decision support to address planning, management, organization, and operational issues. Many advanced technologies were deployed in existing power systems to improve energy efficiency and optimize resource allocation [11].

The development of data- and knowledge-driven technologies has also achieved notable progress. Wang et al. put forward an autonomous intelligent manufacturing system driven by both data and knowledge. Their approach utilized knowledge graphs and digital twins to explore mechanisms such as multi-level autonomous perception, cross-layer and cross-domain cognition, and event-triggered collaborative decision-making. The system aimed to enhance production efficiency in the nonferrous metals sector while effectively tackling issues related to information fragmentation and operational health [12]. Xiao et al. designed a knowledge-driven meta-learning method to address the challenges of deep learning in channel state information feedback enhancement, particularly the need for large volumes of training data and long training times. The meta-model obtained from the meta-training phase enabled the deep learning model to achieve fast convergence when retrained on new scenarios [13]. Wang et al. designed a novel modeling and operation adjustment framework that integrates both data-driven and knowledge-based approaches, aiming to manage the uncertainty of key material attributes and the strong interdependence among variables in multi-unit tablet production. Their method integrated Bayesian networks and case-based reasoning to build a comprehensive framework for the manufacturing process [14]. Yong and Liu put forward a data-driven approach for optimal planning in multimodal visual transmission systems, aiming to tackle the difficulty of formulating the most effective planning strategies under given constraints. Visual features served as the basis for mathematical modeling, while data from other modalities were also introduced to generate optimal planning strategies [15]. Zhu et al. developed a traffic prediction method based on a spatiotemporal graph convolutional network.

Their work addressed the issue that existing studies rarely considered external factors or ignored complex correlations between them. By constructing a knowledge graph for traffic flow prediction, they combined traffic features and knowledge as input to the spatiotemporal graph convolutional backbone network [16].

In summary, existing studies have made progress in power grid fault diagnosis and decision support systems. However, most of them showed limited diagnostic accuracy under complex fault scenarios. Intelligent optimization algorithms based on data and knowledge can address this limitation. Therefore, this study proposes a data- and knowledge-driven power grid fault diagnosis and decision support system. By deeply integrating the precise calculation capabilities of power grid models with logical reasoning, the system aims to achieve accurate diagnosis and precise handling of power grid faults.

3. Fault Diagnosis and Decision Optimization Algorithm Based on Attention Mechanism and Multi-Source Data Integration

3.1. Power grid fault diagnosis method combining 1D-CNN and GWO-LSTM

Existing fault diagnosis methods in power grids rely on manually defined thresholds and fixed rules, which cannot adapt to dynamic changes and noise in complex grid environments. 1D-CNN directly processes raw current signals and automatically extracts high-frequency features in transient faults, providing a more intelligent solution for power grid fault diagnosis [17]. The local receptive property of its convolution kernel allows it to precisely capture microsecond-level mutation signals. The schematic diagram of 1D-CNN is shown in Fig. 1.

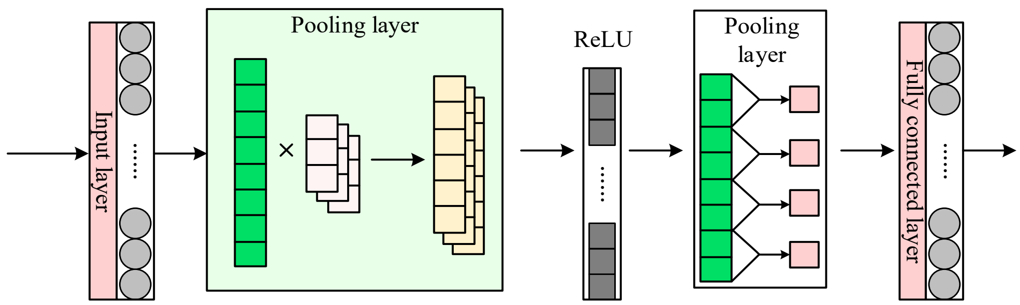

Fig. 1. Schematic diagram of 1D-CNN

Fig. 1 shows how the one-dimensional sequence, together with the convolution kernel, moves along the input sequence to perform inner product computations. By leveraging parameter sharing and local perception, the model extracts local correlation features from the sequence and generates a new feature map. The ReLU layer processes the convolution output by setting negative values to zero and introducing non-linearity, which enhances the model's ability to learn complex sequence patterns. The pooling layer compresses feature dimensions through downsampling, retaining key local information while improving the model's robustness to slight changes in the sequence.The fully connected layer initially transforms the pooled feature maps into a one-dimensional vector by flattening them, then integrates global features and finally generates prediction results through the output node. The convolution process of the CNN is locally applied to the input signal, and its mathematical expression is shown in Equation (1).

$$(I * K)(z,a) = \sum_{m}\sum_{n} I(m,n) \cdot K(z-m,a-n) \tag{1}$$

In Equation (1), I represents the input image, K is the convolution layer, m and n are the sliding window indices of the convolution kernel on the input matrix, z indicates the coordinate position of the output feature map, and a represents the corresponding index of the convolution result. The pooling layer is the downsampling layer in CNN, which reduces the feature map size to lower parameters and computation. Max pooling selects the maximum value in the window to retain significant features and enhance the network's non-linear capacity, as shown in Equation (2).

$$y = \max(x_1, x_2, ..., x_n) \tag{2}$$

In Equation (2), y represents the pooled output value, and x denotes the set of feature values within the pooling window. Although 1D-CNN effectively extracts local features in power grid fault diagnosis, it struggles to model long-term dependencies. LSTM enhances the sequential modeling of fault states and addresses this limitation [18]. However, LSTM is prone to getting stuck in local optima. GWO improves convergence speed and diagnosis accuracy by optimizing LSTM parameters through population-based intelligent search. This forms a more robust data- and knowledge-driven decision system for power grid faults [19,20]. The optimized LSTM using GWO is referred to as GWO-LSTM, and its structure is shown in Fig. 2.

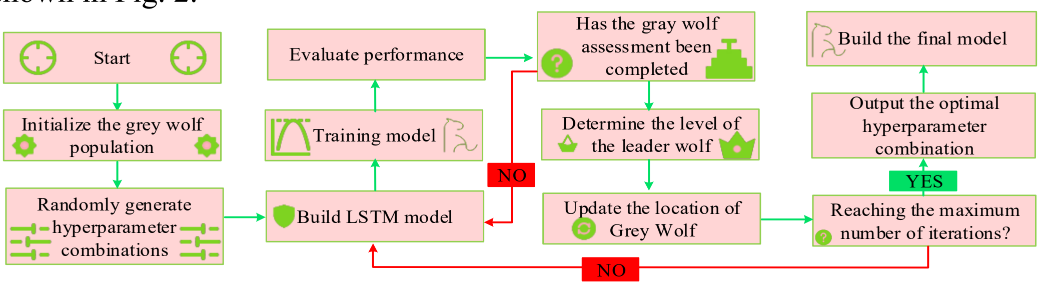

Fig. 2. Structure diagram of GWO-LSTM

In Fig. 2, the LSTM model is built using hyperparameters. The model is trained on a training set, and fitness is evaluated on a validation set. The leader hierarchy is determined based on fitness. Then, hyperparameters are updated using the grey wolf position update mechanism. The iteration continues until the maximum number is reached, and the optimal hyperparameters are used to build the LSTM model, achieving automatic hyperparameter optimization and deep learning model training.Within the LSTM network, the forget gate, input gate, and output gate regulate the process of adding or removing information from the memory cells. Specifically, the forget gate performs selective elimination of irrelevant or redundant information. Its mathematical expression is shown in Equation (3).

$$f_t = \theta(W_f \cdot [h_{t-1}, x_t] + b_f) \tag{3}$$

In Equation (3), f_t represents the output, θ is the sigmoid activation function, W_f denotes the weights, h_t is the output information at iteration t, and b_f represents the bias. Based on this, the study combines 1D-CNN and GWO-LSTM to form the GL-1DCNN. The process flow of the fault diagnosis model based on the GL-1DCNN is shown in Fig. 3.

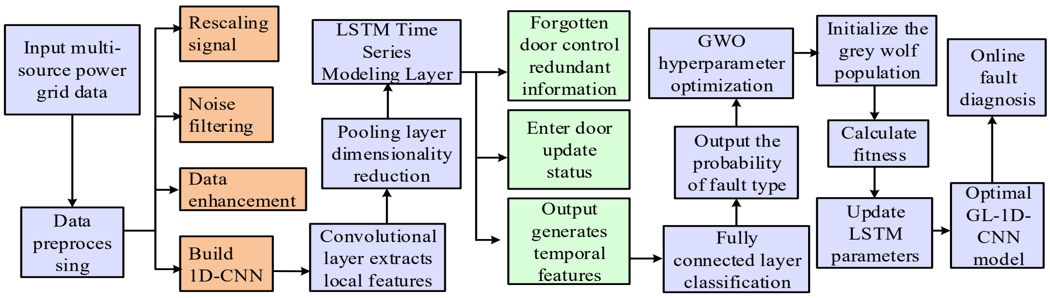

Fig. 3. Flow diagram of power grid fault diagnosis model based on GL-1DCNN algorithm

As shown in Fig. 3, after receiving input from multi-source grid data, the system performs data preprocessing and feeds the data into the convolution layer of the 1D-CNN to extract local features. These features are downsampled through the pooling layer and then input into the LSTM sequence modeling layer. In the LSTM layer, the forget gate controls redundant information, the input gate updates the state, and the output gate generates sequential features. These features are then classified through a fully connected layer. At the same time, the GWO-based hyperparameter optimization process is initiated. The grey wolf population is initialized, fitness is calculated, and LSTM parameters are updated. Through iterative optimization, fitness is recalculated until the parameters converge, achieving online fault diagnosis. The input gate of LSTM adds new information to the memory cell. The equation for the input gate state is shown in Equation (4).

$$S_t = \theta(W_i \cdot [h_{t-1}, x_t] + b_i) \tag{4}$$

In Equation (4), S_t represents the output of the input gate, W_i denotes the weights, and b_i is the bias. The output gate manages the flow of information by employing a sigmoid activation function, while the tanh activation function modulates the state of the memory cell. Together, they determine which parts of the memory cell's content influence the output at the current time step. The equation is shown in Equation (5).

$$o_t = \theta(W_o \cdot [h_{t-1}, x_1] + b_o) \tag{5}$$

In Equation (5), o_t represents the output of the output gate at time t, W_o denotes the output weights, and b_o is the bias term.

3.2. Decision support system based on GL-1DCNN algorithm

Although the GL-1DCNN algorithm performs well in power grid fault diagnosis, it shows limitations in decision support due to insufficient multi-objective coordination. PSO-SVE dynamically balances safety and economic efficiency through multi-objective particle swarm optimization and improves decision transparency and multi-dimensional optimization using a support vector-based interpreter. The process flow of PSO-SVE is shown in Fig. 4.

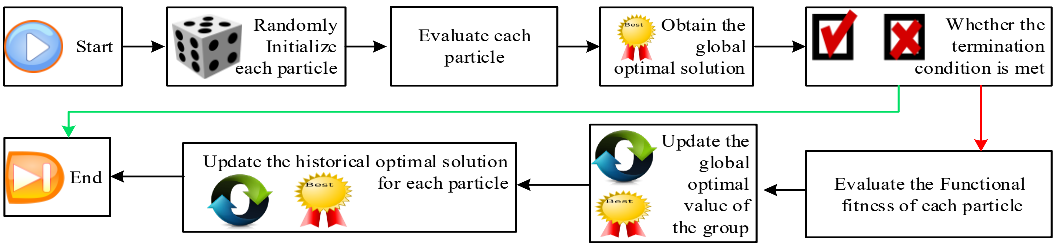

Fig. 4. Process flow of PSO-SVE

In Fig. 4, the PSO-SVE process starts by initializing the particle swarm and randomly generating the initial position of each particle. Next, the algorithm assesses the fitness value of every particle and determines the global best solution. If the stopping criteria are not satisfied, it proceeds to update each particle's velocity and position, reevaluates their fitness values, and revises both the individual and overall optimal solutions accordingly. The process continues until the termination condition is satisfied, and the final optimized result is output. The particle state update for PSO-SVE is shown in Equation (6).

$$V_j = (T+1) = W \cdot V_j(T) + c_1 r_1 (P_{best}(T) - X_j(T)) + c_2 r_2 (G_{best}(T) - X_j(T)) \tag{6}$$

In Equation (6), W represents the inertia weight, c denotes the learning factors, r indicates a random number, $X_j(T)$ is the position vector of a particle, $V_j(T)$ is the velocity vector of the j-th particle at time T, and $P_{best}(T)$ and $G_{best}(T)$ represent the individual and global best position vectors, respectively. The position update expression of PSO-SVE is shown in Equation (7).

$$X_j(T+1) = X_j(T) + V_j(T+1) \tag{7}$$

In Equation (7), $X_j(T+1)$ represents the updated position. The semantic weight mapping expression of PSO-SVE is shown in Equation (8).

$$Y_j(T) = \sigma X_j(T) = \frac{1}{1+e^{-X_j(T)}} \tag{8}$$

In Equation (8), $Y_j(T)$ represents the semantic weight mapping in PSO-SVE. PSO-SVE uses a fitness function to ensure the optimization process considers both general semantic matching and domain knowledge, enabling the decision support system to output results that better align with actual grid operation logic. Therefore, this study integrates PSO-SVE and GL-1DCNN to build a combined decision support system. The process flow is shown in Fig. 5.

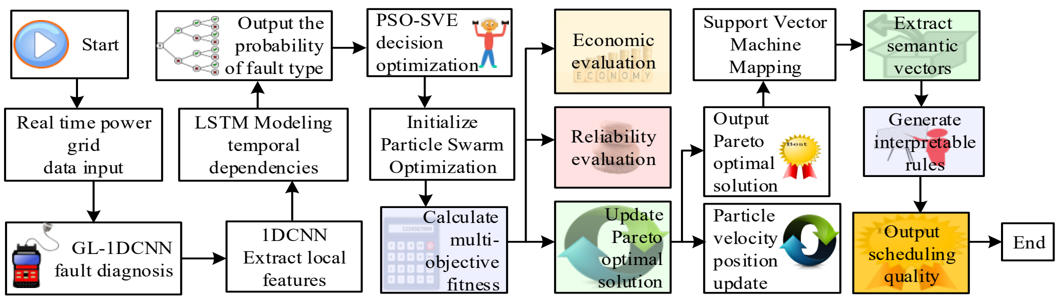

Fig. 5. Decision support system combining PSO-SVE and GL-1DCNN

As shown in Fig. 5, real-time power grid data are first input into the fault diagnosis module. 1D-CNN extracts local features of the fault, and LSTM models the temporal evolution and outputs the fault type and its probability. The diagnosis result is passed to the power grid decision support system, which initializes switch operation and load transfer parameters. A multi-objective fitness function evaluates the safe outage range, economic loss, and recovery time in parallel. The system then iteratively updates the Pareto non-dominated solution set. Finally, through semantic vector analysis, it generates interpretable dispatching rules and outputs feeder isolation instructions and load transfer schemes, completing a closed-loop process from fault diagnosis to decision support. The single-sample semantic vector generation equation in PSO-SVE is shown in Equation (9).

$$V_j = F \odot Y_j \tag{9}$$

In Equation (9), F represents the initial feature vector of the input text, and $\odot$ denotes element-wise multiplication. The temporal semantic vector fusion equation in PSO-SVE is shown in Equation (10).

$$V_j^{seq} = \sum_{k=1}^{N} \gamma^{N-k} \cdot (F_k \odot Y_j) \tag{10}$$

In Equation (10), γ denotes the time decay factor, and F_k represents the feature vector at the k-th time step.

4. Performance Analysis of Intelligent Optimization Model for Power Grid Fault and Decision Based on Multi-Source Data Integration

4.1. Robustness validation of GL-1DCNN algorithm in power grid fault diagnosis

To verify the superiority of the GL-1DCNN algorithm, the study compared it with Attention-1DCNN, Graph Convolutional Network-1D Convolutional Neural Network (GCN-1DCNN), and Residual Network-1D (ResNet-1D). The experimental system used Windows 10 and Linux as operating systems, C++ as the programming language, and 128 GB of memory. In order to ensure the authenticity and reliability of the experiment, the MNIST dataset, Kaggle dataset, microgrid fault detection dataset, EPRI distribution system dataset, and a publicly available transient fault dataset from a certain power company were selected as the experimental datasets. The MNIST dataset is used as the benchmark classification dataset to verify the convergence, robustness, and generalization ability of the proposed algorithm in standard pattern recognition tasks. The Kaggle dataset is collected from multiple actual 10-35 kV distribution network systems, covering radial and ring network structures, including line parameters (such as unit length resistance of 0.1-0.3 Ω/km, reactance of 0.3-0.5 Ω/km), transformer capacity (500-2000 kVA), and load types (industrial, commercial, residential). The data sampling frequency is 10 kHz, including five typical types of faults: three-phase short circuit, single-phase grounding, disconnection, overload, and leakage current. Each data is accompanied by a time-domain waveform, fault type label, and occurrence timestamp. The data scale is about 50000, which has been divided into training set (70%), validation set (20%), and test set (10%). The EPRI dataset is built based on IEEE 13 node, 34 node, and 123 node standard testing systems, with system voltage levels ranging from 4.16 kV to 24.9 kV, including equipment parameters such as lines, transformers, capacitors, and distributed power sources. The data covers operation records under different seasons and load conditions, including voltage, current, active power, reactive power, equipment status, and fault events. The time span exceeds one year, and the total amount of data is about 120000. It is suitable for verifying the adaptability and decision-making effectiveness of the model in standardized power grid structures. The publicly available transient fault dataset of a certain power company is sourced from actual 110 kV transmission systems and 10 kV distribution networks, with system reference voltages of 110 kV and 10 kV, respectively. It includes key electrical parameters such as line parameters, transformer connection groups, and short-circuit capacity. The dataset contains a total of 10000 transient fault records, covering 15 common types of faults such as short circuits, wire breaks, equipment insulation abnormalities, harmonic limit violations, etc. Each data contains waveform data and related protection action information for 5 cycles before and after the fault. The microgrid fault detection dataset is collected from actual power grids in multiple regions, with load types covering industrial, commercial, and residential electricity. The load curve includes different time scales of daily, weekly, and monthly, with a total load capacity range of 1-20 MW and a data volume of 8000 pieces. It is used to evaluate the system's state assessment and early warning capabilities under load fluctuations and new energy access scenarios. All datasets have been preprocessed, including normalization, denoising, segmentation, and annotation, and run in the same experimental environment. The study analyzed the loss values and accuracy of the GL-1DCNN algorithm on both datasets, and the results are shown in Fig. 6.

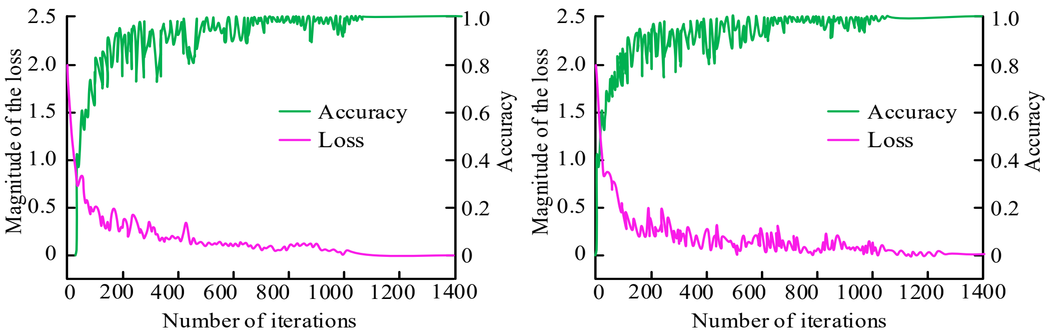

(a) Loss value and accuracy curve chart in MNIST dataset

(b) Loss value and accuracy curve chartKaggle dataset

Fig. 6. Loss and accuracy curves of GL-1DCNN on two datasets

As shown in Fig. 6(a), on the MNIST dataset, the loss curve of the GL-1DCNN algorithm dropped rapidly below 0.3 within the first 200 iterations. The accuracy curve exceeded 0.90 after 150 iterations and stabilized between 0.98 and 1.0 after 200 iterations. As shown in Fig. 6(b), on the Kaggle dataset, the loss curve dropped to about 0.4 after 200 iterations and fluctuated between 0.1 and 0.4 after

800 iterations, eventually converging below 0.1. The average accuracy of GL-1DCNN on the MNIST dataset reached 0.98 with an average loss of 0.11, while on the Kaggle dataset, the average accuracy was 0.97 and the average loss was approximately 0.23. In summary, the GL-1DCNN algorithm demonstrated fast convergence and strong robustness under various conditions. To further validate the effectiveness of the GL-1DCNN algorithm, the study compared the precision-recall curves of the proposed model and the baseline algorithms. The results are shown in Fig. 7.

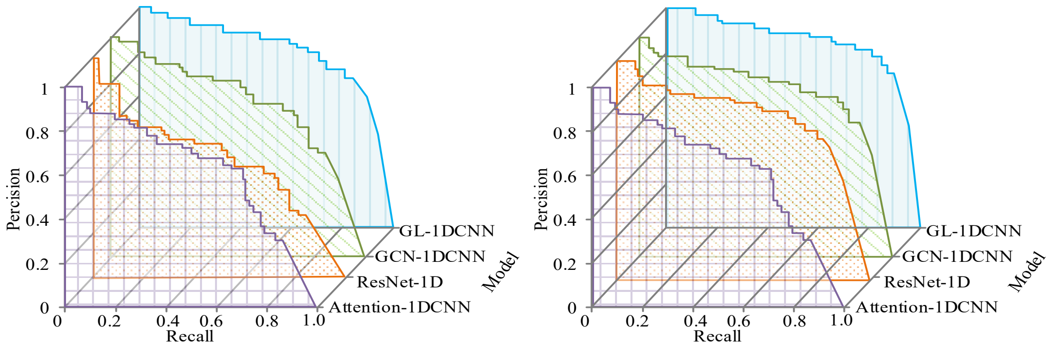

Fig. 7. Precision-recall curve comparison of four algorithms

In Fig. 7, when the recall reached 0.6, the precision of the GL-1DCNN algorithm exceeded 0.7. Even when the recall reached 0.8, its precision remained above 0.6, outperforming the baseline models. For the ResNet-1D algorithm, when the recall reached 0.7, the precision dropped to 0.6 and further decreased to 0.4 when recall reached 0.8. The Attention-1DCNN algorithm achieved 0.7 precision at a recall of 0.5, but the precision dropped to 0.5 when recall increased to 0.7. For the GCN-1DCNN algorithm, precision dropped below 0.6 when the recall was only 0.4. In summary, the GL-1DCNN algorithm maintained high precision under high recall conditions, demonstrating a better balance between matching coverage and accuracy.

4.2. Evaluation and analysis of decision support system combining PSO-SVE and GL-1DCNN

After verifying the performance of GL-1DCNN, the study further evaluated the combined decision support system of PSO-SVE and GL-1DCNN. It was compared with Convolutional Neural Network-Bidirectional Long Short-Term Memory (CNN-BiLSTM), Convolutional Neural Network-Bidirectional Gated Recurrent Unit (CNN-BiGRU), and Particle Swarm Optimization-Deep Belief Network (PSO-DBN). The experiments were conducted using the Pytorch deep learning framework and developed in VS Code. The simulation environment used an AMD Ryzen CPU. The recognition accuracy for five types of power grid faults was tested across all models, and the results are shown in Fig. 8.

A: Short-circuit B: Open-circuit C: Overload D: Grounding E: Leakage current

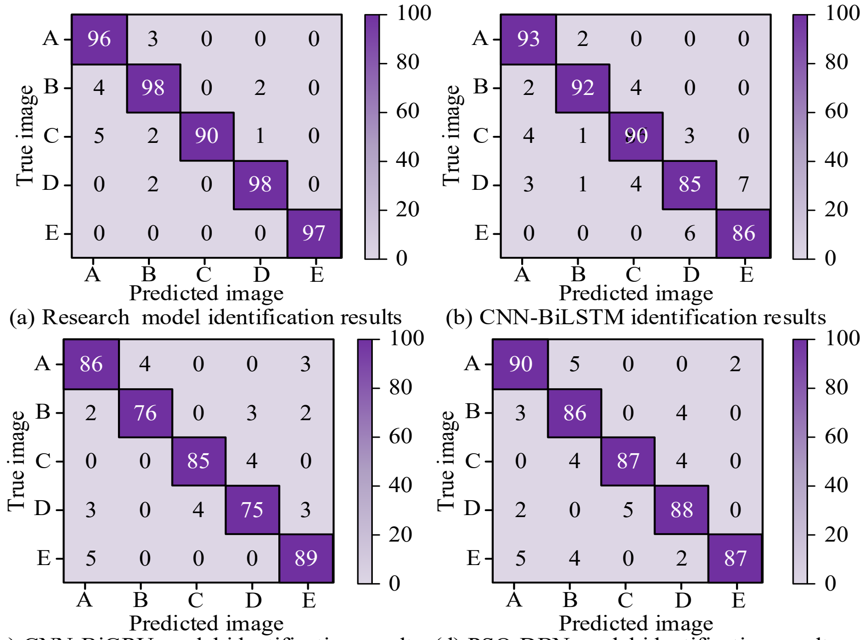

(a) Research model identification results (b) CNN-BiLSTM identification results
(c) CNN-BiGRU model identification results (d) PSO-DBN model identification results

Fig. 8. Prediction results of four models

As shown in Fig. 8, the proposed model achieved a classification accuracy of 96% for short-circuit faults, with only 3% misclassified as open-circuit faults. The recognition accuracy for open-circuit faults reached 98%. For overload faults, the model achieved 90% accuracy with an 8% misclassification rate, outperforming other models. The recognition accuracy for grounding faults reached 98%, and for leakage current faults, it reached 97%. The average correct classification rate for the five fault types was 96%, with a cross-category misclassification rate below 5%, significantly outperforming the baseline models. To further verify the effectiveness of the combined decision support system, the study compared the model's accuracy with the baseline models across different datasets. The results are shown in Fig. 9.

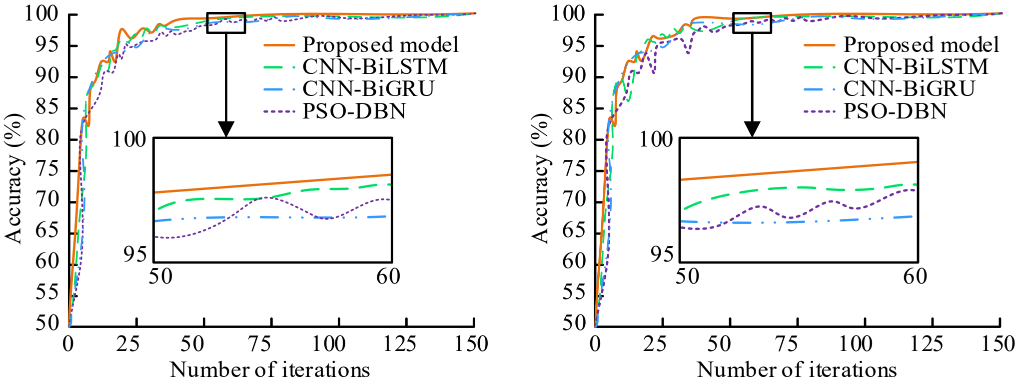

(a) Accuracy on microgrid fault detection dataset (b) Accuracy on EPRI distribution system dataset

Fig. 9. Accuracy comparison of four models

As shown in Fig. 9(a), the combined PSO-SVE and GL-1DCNN decision support system achieved an accuracy of 97.5% between 50 and 60 iterations on the microgrid fault detection dataset. As shown in Fig. 9(b), it achieved an accuracy of 98% on the EPRI distribution system dataset. Both trends remained stable and outperformed the baseline models. In summary, the combined PSO-SVE and GL-1DCNN decision support system achieved fast convergence, high precision, and strong robustness across different scenarios. It produced high-accuracy results for power grid fault diagnosis in real time, offering more reliable support for real-time decision-making. To further verify the accuracy of the proposed model, the study conducted experiments using two real-world power grid datasets. Accuracy was denoted as Ac., response time as Re., and CPU usage as CPU. The results are given in Table 1.

Table 1

Results of load forecasting, fault warning, and grid state assessment

Test project		Load Forecasting			Fault warning			Power grid status assessment		
Model	Data	Ac.	Re.	CPU.	Ac.	Re.	CPU.	Ac.	Re.	CPU.
Proposed model	1	93	120	30	97	85	23	95	110	32
	2	95	125	25	93	135	12	95	120	30
CNN-BiLSTM	1	86	200	65	86	260	56	86	230	65
	2	84	230	45	74	350	45	86	360	45
CNN-BiGRU	1	82	240	62	85	255	86	82	250	52
	2	85	350	75	85	320	64	87	340	35
PSO-DBN	1	81	450	58	75	450	63	89	420	48
	2	85	250	65	82	280	49	85	230	59

In Table 1, on both real-world datasets, the proposed model showed clear advantages over the baseline models in three core tasks: load forecasting, fault warning, and grid state assessment. For load forecasting, the model achieved an accuracy of 93% and 95%, respectively. For fault warning, it reached 97% and 93%. For grid state assessment, it achieved 95% accuracy on both datasets. The average accuracy across all tasks was 94%, with an average response time of 116 ms and an average CPU usage of 26%. In conclusion, the proposed model provided accurate support for real-time grid monitoring and decision-making and significantly outperformed the baseline models.

5. Conclusion

In view of the problem that the current traditional power grid fault diagnosis and decision support system relies on a single data source, which leads to low reliability of prediction results, this study innovatively proposed a decision support system combining PSO-SVE and GL-1DCNN and solved the problem of insufficient utilization of multi-source data through a data-knowledge dual-driven architecture. The experimental results show that the average correct classification rate of the research model for five types of faults is 96%, the average accuracy in various businesses is 94%, the average response time is 116 ms, and the average CPU usage is 26%. In summary, the newly developed algorithm of the institute can reduce the fault response time, enhance the stability of power grid operation, and effectively overcome the current traditional means of dealing with complex fault situations. The problems of low diagnostic accuracy and delayed response speed caused by insufficient information integration. Promote the operation of the power grid to move towards a more intelligent direction. Although the research model performs well in multi-source data fusion and knowledge collaborative decision-making, there are still problems such as insufficient sample coverage, knowledge graph update bottlenecks and edge node costs. It is hoped that data enhancement technology will be deepened in the future to continuously improve the engineering universality and real-time response of the system.

Acknowledgments

This work was supported by the Research and Application of Power Grid Abnormal Scheduling Decision Technology Driven by Data and Knowledge Collaboration, with the project number 000005KC24010014 (Science and Technology Project number: ZDKJXM20240015).

REFERENCES

[1] Zhang X, Ning H. Transformer fault diagnosis method based on relieff and HPO-SVM[J]. University Politehnica of Bucharest Scientific Bulletin Series C-Electri Eng Comput Sci, 2023, 85(3): 137-152.

[2] Zhao D, Jiang R, Feng M, Yang J, Wang Y, Hou X, Wang X. A deep learning algorithm based on 1D CNN-LSTM for automatic sleep staging. Technology and Health Care, 2022,

30(2): 323-336.

[3] Yang L, Xu M, Guo Y, Deng X, Gao F, Guan Z. Hierarchical Bayesian LSTM for head trajectory prediction on omnidirectional images. IEEE Transactions on Pattern Analysis and Machine Intelligence, 2021, 44(11): 7563-7580.

[4] Yun Y, Gen M, Erdene T N. Applying GA-PSO-TLBO approach to engineering optimization problems. Math. Biosci. Eng, 2023, 20(1): 552-571.

[5] Wang Y, Shi C, Guo D, Chen S, Zhong Z, Wang K. Research on control strategy of power grid simulator based on predictive control[J]. University Politehnica of Bucharest Scientific Bulletin Series C-Electri Eng Comput Sci, 2025, 87(3): 387-402.

[6] Gheisari M, Hamidpour H, Liu Y, Saedi P, Raza A, Jalili A, Rokhsati H, Amin R. Data Mining Techniques for Web Mining: A Survey. Artificial Intelligence and Applications, 2023, 1(1): 3-10.

[7] Almulhim T S, Barahona I. Decision support system for ranking relevant indicators for reopening strategies following COVID-19 lockdowns. Quality & quantity, 2022, 56(2): 463-491.

[8] Shahraki N, Sir M Y, Prindle T, et al. A decision-support system to schedule rotations for trainees. ATS scholar, 2022, 3(3): 425-432.

[9] Bazilevych KO, Chumachenko DI, Hulianytskyi LF, Meniailov IS, Yakovlev SV. Intelligent decision-support system for epidemiological diagnostics. I. A concept of architecture design. Cybernetics and Systems Analysis, 2022, 58(3): 343-353.

[10] Lu Y. A knowledge-driven decision support system for remote medical management. Mathematical Biosciences and Engineering, 2023, 20(2): 2732-2749.

[11] Mufana M W, Ibrahim A. Implementation of smart grid decision support systems. IDOSR Journal of Scientific Research, 2022, 7(1): 50-57.

[12] Wang H, Wang C, Liu Q, Zhang X, Liu M, Yumin M, Yan F, Shen W. A data and knowledge driven autonomous intelligent manufacturing system for intelligent factories. Journal of Manufacturing Systems, 2024, 74: 512-526.

[13] Xiao H, Tian W, Liu W, Guo J, Zhang Z, Jin S. Knowledge-driven meta-learning for CSI feedback. IEEE Transactions on Wireless Communications, 2023, 23(6): 5694-5709.

[14] Wang Z, Tang S, Yang Y, Chen Y, Yang L. Data-Knowledge-Driven Modeling and Operational Adjustment for the Pharmaceutical Tablet Manufacturing Process via Wet Granulation. ACS omega, 2023, 8(27): 24441-24453.

[15] Yong J, Liu K. A knowledge and data-driven optimal planning scheme for multi-modal vision transmission systems. Mathematical Biosciences and Engineering, 2023, 20(7): 11939-11956.

[16] Zhu J, Han X, Deng H, Tao C, Zhao L, Wang P. KST-GCN: A knowledge-driven spatial-temporal graph convolutional network for traffic forecasting. IEEE Transactions on Intelligent Transportation Systems, 2022, 23(9): 15055-15065.

[17] Sabor N, Gendy G, Mohammed H, Wang G, Lian Y. Robust arrhythmia classification based on QRS detection and a compact 1D-CNN for wearable ECG devices. IEEE Journal of Biomedical and Health Informatics, 2022, 26(12): 5918-5929.

[18] Bao T, Wang C, Yang P, Xie SQ, Zhang ZQ, Zhou P. LSTM-AE for domain shift quantification in cross-day upper-limb motion estimation using surface electromyography. IEEE Transactions on Neural Systems and Rehabilitation Engineering, 2023, 31: 2570-2580.

[19] Bommidi B S, Teeparthi K, Dulla Mallesham V K. ICEEMDAN-Informer-GWO: a hybrid

model for accurate wind speed prediction. Environmental Science and Pollution Research, 2024, 31(23): 34056-34081.

[20] Jadda A, Prabha I S. Adaptive Weiner filtering with AR-GWO based optimized fuzzy wavelet neural network for enhanced speech enhancement. Multimedia Tools and Applications, 2023, 82(16): 24101-24125.